20th Australasian Fluid Mechanics Conference
Perth, Australia
5-8 December 2016

Aero-acoustic simulations of an empty cavity

V. Zecevic[1], J. A. Geoghegan[1], B. Thornber[1], G. A. Vio[1]

[1]School of Aerospace, Mechanical and Mechatronic Engineering
The University of Sydney, NSW 2006, Australia

Abstract

Simulations of an empty cavity are performed in three dimensions at a Mach number of 0.8 typical of aeronautical applications using a finite volume large eddy simulation (LES) code Flamenco which uses up to fifth order spatial reconstructions in advective terms and a HLLC Riemann solver. The primary motivation is predicting aero-acoustic loads within the cavity as well as any store which may be inside. Our results are compared to published experimental and numerical data. Our research ultimately aims to use fully coupled fluid structure interaction techniques to simulate this problem as well as a more complicated problem with a captive store with this work addressing the ability of our computational techniques to satisfactorily predict the aero-acoustic properties of the simplified problem. We explore the influence of grid resolution, sampling time and frequency resolution. Power spectral densities of pressure obtained from our calculations agree well with published experimental results.

Introduction

The study of compressible flow over open cavities has been a prominent area of research in the field of aero-acoustics since the seminal experimental work by Rossiter [8] in 1964. Most of the work in this field deals with the identification and control of the complex unsteady flow fields generated by the interaction of turbulent fluctuations and the free shear layer. It was shown that for rectangular geometries, the cavity produced intense aero-acoustic loading leading to cavity resonance with sound pressure levels (SPL) reaching 120 dB [5]. The work of Rossiter provided a semi-empirical model for predicting the frequencies of the resonant cavity modes, however it fails to accurately resolve the mode shapes, or peak amplitudes. In the application of these open cavities to aircraft storage bays, the ability to predict the unsteady flow field structure is paramount to maintaining the integrity of the captive stores within. Despite the potential for the aero-acoustic loading generated by the cavity to lead to catastrophic failure of the store itself and the release mechanism, up until recently there has been little work conducted in analysing the effects of a captive store and the fluid-structure interaction (FSI).

More recently, there have been several papers produced by Sandia National Laboratories which have covered both the experimental and numerical simulations of rectangular geometry cavities with and without generic captive stores. Barone and Arunajatesan [3] presented results for the unsteady pressure loadings within a cavity with and without a store using a hybrid Reynolds-averaged Navier Stokes/ Large Eddy Simulation (RANS/LES) solver at transonic mach numbers. These results demonstrated the ability to resolve the single-point cavity wall pressure spectra within 2-3 dB amplitude and 5% frequency across the majority of the resonant tones. However there were large inaccuracies in the prediction of the store accelerations. It was also identified in this paper that the flow field structure differs significantly due to the presence of the store, which interferes with the free shear layer. Further work by Arunajatesan *et. al.* [2, 1] focused on the FSI framework for predicting the structural loading of a rigid store through a one-way coupling mechanism. This development however did not capture the flow field disturbances generated by a vibrating store within the cavity. There has been significant experimental work concerning the FSI of stores in cavities by Wagner et. al. [12, 13] exploring among other things the effects of store vibration on the acoustic spectra within the cavity.

The focus of this paper is evaluating the ability of our numerical method to predict the sound pressure spectra for a rectangular cavity. In particular we will verify that the simplifying approximations we have made such as laminar inflow and using a coarse mesh to damp reflections maintain the ability to accurately predict the spectra. We explore the influence of grid resolution, sampling time and frequency resolution on the results. Power spectral densities of pressure obtained from our calculations agree well with published experimental results.

Simulation Method

Simulations were performed using Flamenco, a compressible large eddy simulation (LES) code with fifth order spatial discretization and strong stability preserving, second order explicit Runge-Kutta time stepping. The code uses the HLLC Riemann solver and implicit LES which has been shown to be an effecive method of subgrid turbulence modelling [9, 11, 6, 7]. The simulations have been performed using three grid sizes which are all relatively coarse in terms of the grid spacing in the boundary layer along the roof of the cavity. The decision to use a coarse grid was made based upon considerations of computational feasibility. The primary goal of these simulations has been to accurately predict acoustic power spectral density (PSD) plots at locations within the cavity, in order to reduce statistical noise to acceptable levels while maintaining sufficient frequency resolution in these plots, simulations must be long running. We have found that a sampling time of 100 ms is marginally acceptable with 200 to 1000 ms being more suitable. We will compare our computed PSD plots to results from Barone and Arunajatesan [4] whose experimental results use a sampling time of 1000 ms and numerical simulations use a sampling time of 100 ms. Thus since the number of time steps and hence processor time required to reach this physical time is inversely proportional to the Courant number, there is a trade of between grid resolution and sampling time possible with a given amount of processing time. Despite the under-resolved boundary layer in the wind tunnel, we have found reasonable agreement to experimental results.

The domain consists of a wind tunnel with a cavity whose dimensions are $l_x = 8$in, $l_y = 4$in $l_z = 1.5$in in the roof. The streamwise x direction is normal to the incoming flow, the spanwise direction is aligned with the y axis and z is the wall normal direction. The grid is uniform within the cavity and also within an adjacent 10" by 6" by 1" fine region within the tunnel. The tunnel walls are located 0.7m away from the cavity, as are the inlet and outlet. The mesh within the tunnel then grows with a growth rate of 1.07 away from the fine region. The grid size in the regions furthest away from the cavity at the entrance, exit and other walls of the wind tunnel is sufficiently large that numerical dissipation significantly damps out reflections. The

Mesh name	$n_{x,cav}$	$n_{y,cav}$	$n_{z,cav}$	n_{tot}
coarse	192	96	28	4,057,088
normal	240	120	35	8,418,000
fine	304	152	44	15,887,872

Table 1: Coarse, normal and fine mesh dimensions used.

distance of these features from the cavity also ensure that reflections are sufficiently damped. Symmetry boundary conditions are used at all tunnel boundaries except for the wall adjacent to the cavity which uses a wall boundary condition. The inlet and outlet use inflow and outflow boundary conditions respectively.

The initial conditions are air at a temperature of 298 K, pressure of 101.325 kPa and a freestream velocity of 276.85 m/s resulting in a Mach number of 0.8 with a boundary layer thickness of 0.014605 m or 0.575" at the wall adjacent to the cavity. Using the initial boundary layer thickness δ and approximating the wall shear using the Schlichting correlation, the Reynolds numbers based on boundary layer thickness is $\mathrm{Re}_\delta = 260,864$ and the characteristic wall distance based on wall shear is $z_\tau = 1.142 \times 10^{-3}$ mm leading to boundary layer z^+ values over 700 even for the finest mesh, here z is the wall normal direction and z^+ is the distance of the first node from the wall in wall units. Thus the boundary layer is essentially unresolved. The initial conditions are unperturbed and turbulence is generated by fluid instabilities generated within the cavity itself. As a consequence, there is no turbulence upstream of the cavity. Despite the incomplete representation of the boundary layer turbulence, the aero-acoustic properties of the cavity are remarkably well predicted as will be shown in the results. The time steps used are calculated based on a desired Courant number of 0.5 as shown in Table 2, in order to reach a simulation time of 180 ms using the fine grid we have had to run for around 340,000 time steps. Assuming a hypothetical situation where the boundary layer was fully resolved into the viscous sublayer, the resulting 100 fold reduction in time step size would require 34 million time steps to reach a marginal statistical sample, a computational effort that is beyond feasible with our resources. Grid dimensions within the cavity for our three tested grids are shown in Table. 1. A diagram of the mesh itself in the xz plane is shown in Figure 1.

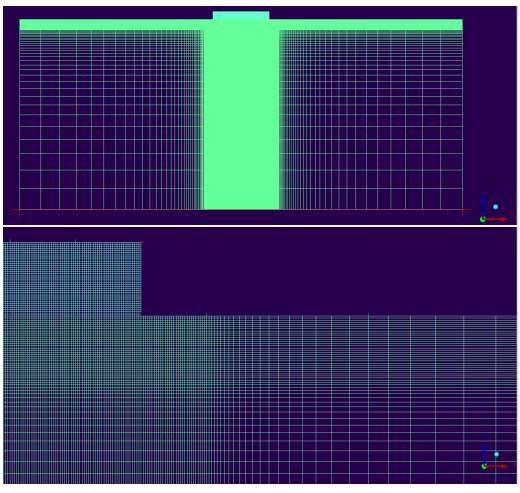

Figure 1: Mesh plots in the xz plane, showing uniform grid within cavity and fine region surrounding the cavity followed by growth region in tunnel.

The structured multi-block mesh was developed using Tcl scripting and ICEM CFD. The total number of blocks used was 452, this amount of splitting was sufficient to obtain acceptable parallel efficiency up to 256 processors. The block splitting strategy can be seen in Figure 3 and Figure 2.

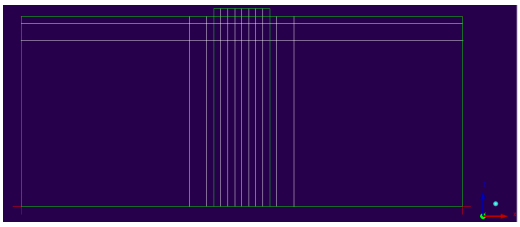

Figure 2: Block splitting in the xz plane.

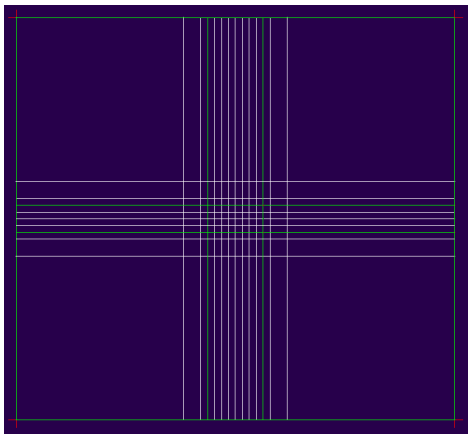

Figure 3: Block splitting in the xy plane.

Mesh name	Δx_{cav} (mm)	Δt (s)	z^+
coarse	1.06	8.50×10^{-7}	929
normal	0.847	6.80×10^{-7}	742
fine	0.668	5.37×10^{-7}	584

Table 2: Coarse, normal and fine mesh grid spacing, time step and z^+ values.

The PSD's are calculated using Welch's periodogram method with 75% overlap. We have used the Nutall window function in order to improve the accuracy of the averaged spectra.

Results

The main results of importance are the acoustic PSD plots as shown in Figure 7, Figure 8 and Figure 9. We also show parallel scaling in Table 3, this table demonstrates that the block subdivision was sufficient to obtain reasonable scaling up to 256 processors however the parallel efficiency of 75% at that stage indicates that more careful block splitting would be beneficial if more processors were used. Some flow visualizations demonstrating characteristic momentum, pressure and temperature fields are shown in Figure 4, Figure 5 and Figure 6 respectively.

All of the PSD results shown in this section are overlayed with the results of Barone and Arunajatesan [4], the black line labeled 'Expt.' corresponds to their experimental results and the red line labelled 'SigmaCFD' corresponds to their numerical results. Figure 7 shows a comparison between 25 Hz and 50 Hz frequency resolutions used in the calculation of the PSD. These results are obtained using the normal grid and 176 ms of sam-

Processors	Time per step (s)	Updates rate per processor (kups)	Efficiency
4	203	19.6	100%
8	110	18.1	92%
16	54.0	18.4	94%
32	27.2	18.2	93%
64	15.6	15.9	81%
128	7.81	15.9	81%
256	4.17	14.9	76%

Table 3: Parallel scaling of fine grid simulations, wall time per time step, per processor update rate in kilo updates per second and parallel efficiency are shown.

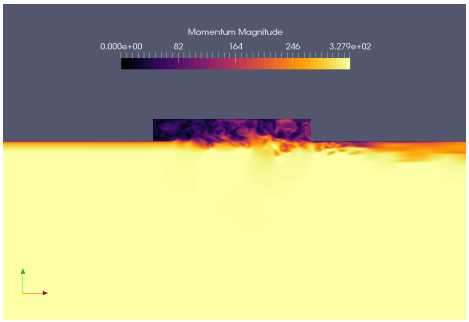

Figure 4: Momentum field visualization.

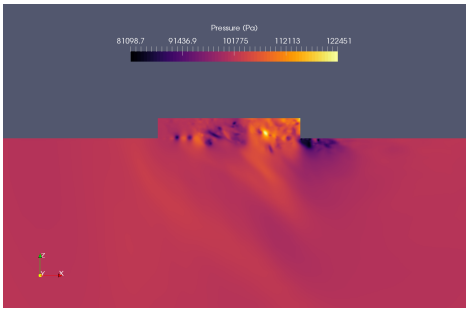

Figure 5: Pressure field visualization.

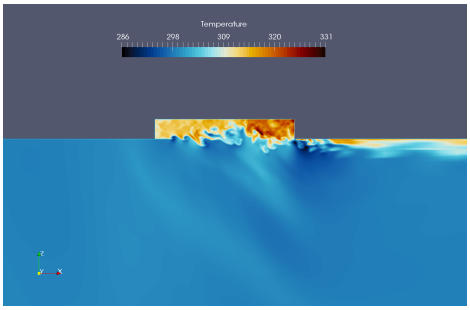

Figure 6: Temperature field visualization.

ple time. The finer frequency resolution plot shows more detail however is more noisy and would require further sampling time in order to reduce noise to an accaptable level. 50 Hz frequency resolution is sufficient to show the relevant peaks in the PSD however given enough sampling time, 25 Hz or finer resolution would be preferable.

Figure 8 shows a comparison between 88 ms of sampling time and 176 ms of sampling time using our normal grid and 50 Hz frequency resolution. There is a clear improvement in the results with significantly less noise as sample time is increased. Even 176 ms, while better than our 76 ms results and the 100 ms numerical results of [4] still shows fluctuations which would be reduced given further time. The experimental results of [4] which use a 10 Hz frequency resolution and 1000 ms of sample time represent truly well resolved and statistically averaged results and can be considered a goal for numerical simulations to reach.

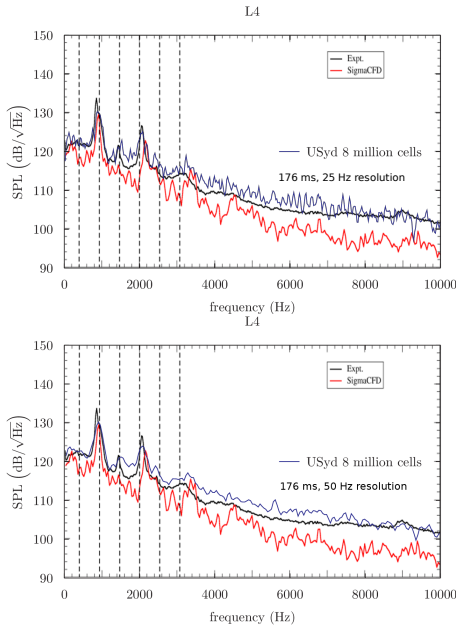

Figure 7: Frequency resolution comparison, image overlay Barone and Arunajatesan [4] .

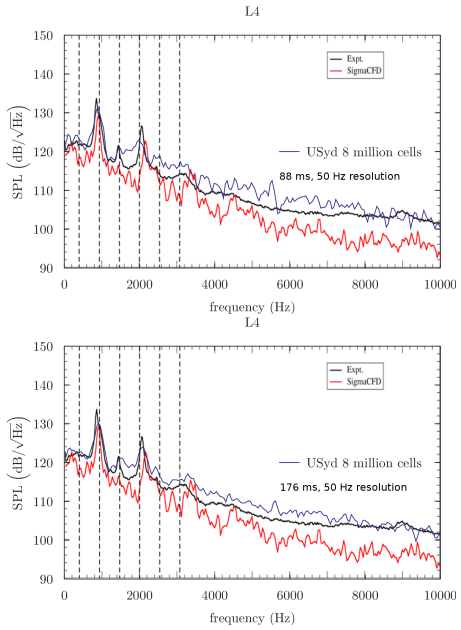

Figure 8: Sample time comparison, image overlay Barone and Arunajatesan [4].

Figure 9 compares 100 ms sample time and 50 Hz frequency resolution spectra using all three grid resolutions. It is expected that errors between numerical simulations and experiment will reduce with grid size. Unfortunately in this case, the opposite

trend is apparent. Our best agreement is found using the coarsest mesh. The coarse mesh results predict the lowest frequency mode amplitude almost exactly, the normal grid under predicts by 4 dB and the fine grid under predicts by 8 dB. The prediction of other mode amplitudes doesn't follow a clear trend with grid size, for example the third node is well predicted by the coarse and fine grids but is under predicted by 6 dB using the normal grid. We could state that our coarse grid simulation predicts the amplitudes of the first three modes within 2 dB however in order for these results to be considered robust and used for predictive purposes, they would need to improve with increased grid resolution. At this stage we hypothesise that there are two issues at play, firstly more sample time is required, as shown in Figure 8, the prediction of peak amplitude improves when sample time is increased from 76 ms to 176 ms, secondly there is some source of error which is causing the under prediction of the first mode amplitude as grid resolution is increased. We note that Figure 8 does not show an improvement in the prediction of the amplitude of the first mode with increased sample time, this indicates that another factor is in play.

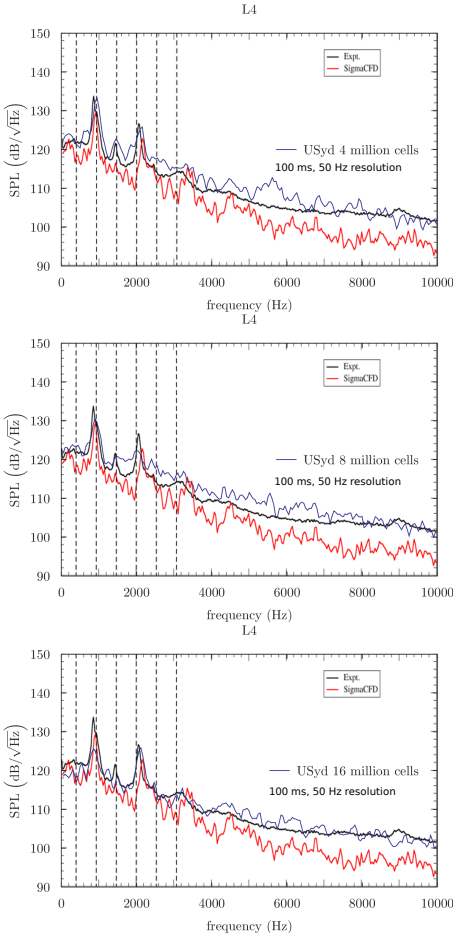

Figure 9: Grid resolution comparison, image overlay Barone and Arunajatesan [4].

Conclusions

We have performed numerical simulations of the specified cavity configuration at a Mach number of 0.8 and found good agreement with experimental results. In particular, our coarse grid simulations predict the amplitude of the first three modes within 2 dB. We have determined that a sampling time of 100 ms and resolution of 50 Hz is marginally acceptable and that improved results would be obtained using sampling time up to 400 ms with a frequency resolution of 25 Hz. Future work will be to extend these simulations to the longer sampling time, determine the source of error present in our higher resolution simulations and explore the effects of different aspect ratios and potentially captive stores.

Acknowledgements

The authors would like to acknowledge Dr Matteo Giacobello and the Defence Science and Technology Group Australia for the support in this project.

References

[1] Arunajatesan, S., *et al.*, One-way coupled fluid structure simulations of stores in weapons bays, in *51st AIAA Aerospace Sciences Meeting*, Grapevine, TX, United states, 2013.

[2] Arunajatesan, S., *et al.*, Validation of an FSI modeling framework for internal captive carriage applications, in *19th AIAA/CEAS Aeroacoustics Conference*, Berlin, Germany, 2013.

[3] Barone, M. and Arunajatesan, S., Pressure loading within rectangular cavities with and without a captive store, in *52nd AIAA Aerospace Sciences Meeting*, National Harbor, MD, United States, 2014.

[4] Barone, M. F. and Arunajatesan, S., A computational study of flow within cavities with complex geometric features, in *53rd AIAA Aerospace Sciences Meeting*, Kissimmee, Florida, 2015.

[5] Dix, R. and Bauer, R., Experimental and predicted acoustic amplitudes in a rectangular cavity, in *38th AIAA Aerospace Sciences Meeting*, American Institute of Aeronautics and Astronautics (AIAA), 2000.

[6] Drikakis, D.,*et al.*, Large eddy simulation using high-resolution and high-order methods *Phil. Trans. R. Soc. A: Mathematical, Physical and Engineering Sciences*, **367**(1899), 2009, 2985-2997.

[7] Garcia-Uceda Juarez, A., *et al.*, Steady turbulent flow computations using a low Mach fully compressible scheme *AIAA Journal*, **52**(11), 2014, 2559-2575.

[8] Rossiter, J. E., Wind tunnel experiments on the flow over rectangular cavities at subsonic and transonic speeds, Technical Report 3438, Royal Aircraft Establishment, 1964.

[9] Thornber, B., *et al.*, On the implicit large eddy simulations of homogeneous decaying turbulence, *J. Comput. Phys.*, **226**, 2007, 1902–1929.

[10] Thornber, B., *et al.*, An improved reconstruction method for compressible flows with low Mach number features *J. of Comput. Phys.*, **227**(10), 2008, 4873-4894.

[11] Thornber, B., Drikakis, D., Implicit large-eddy simulation of a deep cavity using high-resolution methods *AIAA Journal*, **46**(10), 2008, 2634-2645.

[12] Wagner, J. L., *et al.*, Response of a store with tunable natural frequencies in compressible cavity flow, *AIAA. J.*, **54**, 2016, 2351–2360.

[13] Wagner, J. L., *et al.*, Fluid-structure interactions in compressible cavity flows, *Phys. Fluids*, **27**.